NASA TECHNICAL NOTE

NASA TN D-5357

c. 1

NASA TN D-5357

OPTICAL SIMULATION OF A RADIO-ASTRONOMY INTERFEROMETER EXPERIMENT

by James P. Strong III

Goddard Space Flight Center
Greenbelt, Md.

NATIONAL AERONAUTICS AND SPACE ADMINISTRATION • WASHINGTON, D. C. • SEPTEMBER 1969

OPTICAL SIMULATION OF A RADIO-ASTRONOMY INTERFEROMETER EXPERIMENT

By James P. Strong III

Goddard Space Flight Center
Greenbelt, Md.

NATIONAL AERONAUTICS AND SPACE ADMINISTRATION

For sale by the Clearinghouse for Federal Scientific and Technical Information
Springfield, Virginia 22151 – CFSTI price $3.00

ABSTRACT

A laser technique has been used to simulate processed output from a proposed spaceborne radio-astronomy interferometer experiment comprising two satellites separated by a controlled distance. The experiment effectively transmits the Fourier transform of the radio stars over the celestial sphere. The Fourier transform is a function of the distance between the two satellites and of the direction of the line connecting them. The existence of upper and lower bounds on the distance between the satellites creates voids in the Fourier transform space, causing resolution problems in the reconstruction of the star pattern on the ground from the Fourier transform. Because coherent optical techniques can obtain the two-dimensional Fourier transform, they can be used to simulate the proposed experiment. Optical filters can be made which represent the voids in the Fourier transform of the star pattern. An inverse transform shows the effects of the filtering, simulating the effects of the voids. This paper discusses optical filtering in general and the particular optical system used. Results are shown for 1-MHz and 10-MHz RF sources, representing the worst and the best resolution expected.

Two conclusions are drawn. First, optical techniques are excellent for problems of this type. Second, because of the poor resolution in the 1-MHz range, 3,000 meters (the proposed maximum distance between the two satellites) is inadequate.

CONTENTS

OPTICAL SIMULATION OF A RADIO-ASTRONOMY INTERFEROMETER EXPERIMENT

by

James P. Strong III

Goddard Space Flight Center

INTRODUCTION

Coherent optical processing is a very powerful tool for making "spatial" frequency analyses of two-dimensional data. Optical techniques can produce a two-dimensional Fourier transform of the data which is a "spatial" frequency analysis. One can subsequently produce an inverse Fourier transform to reproduce the original data. Filters can be introduced which attenuate certain "spatial" frequencies of the Fourier transform. Taking the inverse Fourier transform will then show the effects of the filtering on the original data. This property of optical processing has made it useful in simulating a proposed spaceborne radio-astronomy interferometer experiment.

This proposed experiment will attempt to make a 1- to 10-MHz RF map of the celestial sphere. For this purpose, two satellites will be placed side by side in the same orbit. Each will receive signals from astronomical radio sources, along with background noise. The received signal from one satellite (the maneuvering satellite) will be transmitted to the other (the reference satellite). The two signals, bandpass-filtered at the RF frequency under consideration, will be fed to a cross-correlator. Dr. E.J. Lueke, in a private communication, has derived the output of the cross correlator, C (N), as:

$$C(\mathbf{N}) = \iiint_{\mathbf{P}} D(\mathbf{P})\ e^{-j\,(\mathbf{P}\cdot\mathbf{N})}\, d\,\mathbf{P} \tag{1}$$

P is a three-dimensional vector whose direction is from the two satellites to the RF sources (stars), as shown in Figure 1. The magnitude of **P** is between zero and 1. $D(\mathbf{P})$ is the brightness function of the RF sources over a unit celestial sphere. $D(\mathbf{P})$ has values only at $|\mathbf{P}| = 1$. **N** is a vector whose direction coincides with a line connecting the two satellites. Its magnitude is proportional to the distance between the two satellites and to the RF source frequency under consideration. If one considers Equation 1, it

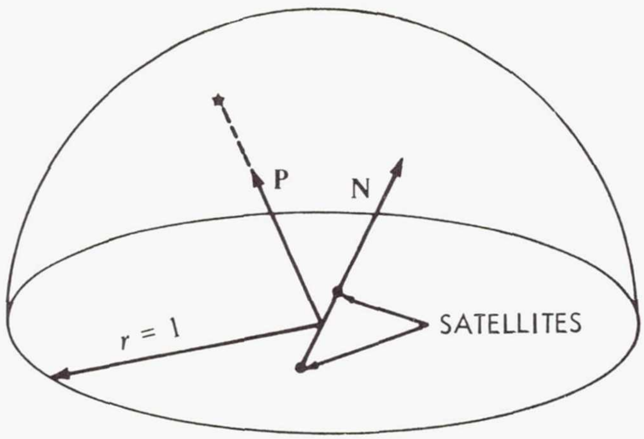

Figure 1 — Unit radius celestial sphere of interferometer experiment.

will be noted that $C(\mathbf{N})$ is the three-dimensional spatial Fourier transform of the brightness function $D(\mathbf{P})$. When $C(\mathbf{N})$ is relayed back to earth, the inverse Fourier transform can be taken to obtain:

$$D(\mathbf{P}) = \iiint_{\mathbf{N}} C(\mathbf{N})\, e^{j(\mathbf{P}\cdot\mathbf{N})}\, d\mathbf{N} \quad . \qquad (2)$$

There are several difficulties in obtaining the inverse Fourier transform. The one that concerns us the most is that **N** is limited in magnitude, since the two satellites can be neither infinitely far apart nor on top of one another. The proposed size of the antennas on each satellite limits the minimum separation to about 300 meters. It is expected that limited transmitter power for communications between the satellites will hold their maximum separation to about 3,000 meters. This limit places a restriction on the bandwidth of **N**, thereby reducing the resolution of $D(\mathbf{P})$.

An optical correlator is an ideal tool to exhibit the results of the limitations on $|\mathbf{N}|$. It provides the experimenter with a photograph of a simulated RF celestial map showing the limits of resolution.

The body of this paper will discuss the optically generated two-dimensional Fourier transform and how the transform can be used to simulate the magnitude limitations on **N**. It will then show, on a two-dimensional equivalent of an RF source map, the results of these limitations.

OPTICAL FILTERING

The optical experiment was set up as shown in Figure 2, where f_1 and f_2 are the focal lengths of lens 1 and lens 2, respectively. If a transparency (for example, a star pattern) is placed at A, its

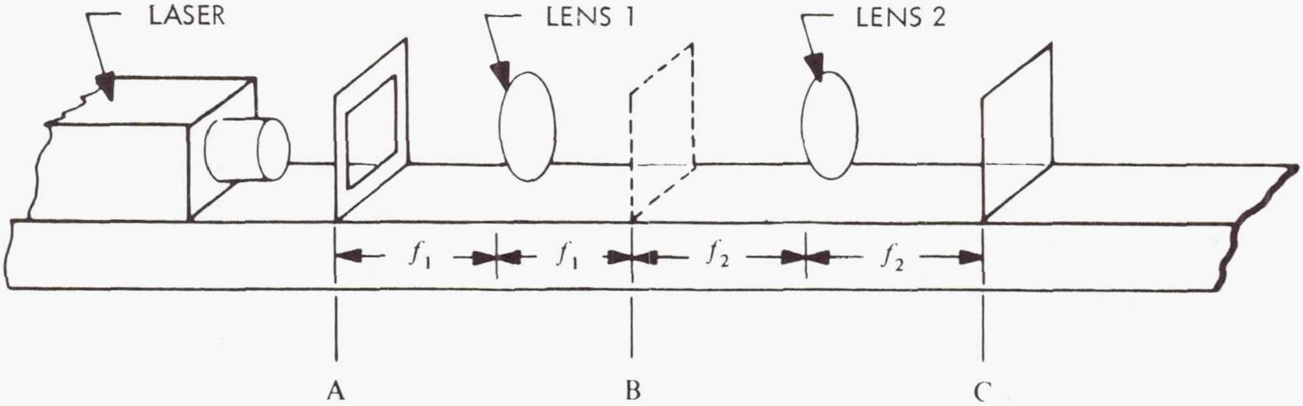

Figure 2 — Coherent optical arrangement for obtaining Fourier transform and inverse.

two-dimensional Fourier transform will appear on a screen placed at B. If the screen is removed, lens 2 causes the inverse transform to appear on a screen placed at C. Thus, the Fourier transform of the Fourier transform at B produces the original image again at C. With this arrangement, one may place in the Fourier transform plane at B a mask which would attenuate certain regions of the transform plane. The results of this masking on the original image may be observed at C. This procedure is analogous to passing a signal through a filter and observing the output waveform.

Let us now discuss the Fourier transform plane and see the results of masking. Figure 3 shows a two-dimensional Fourier transform plane.

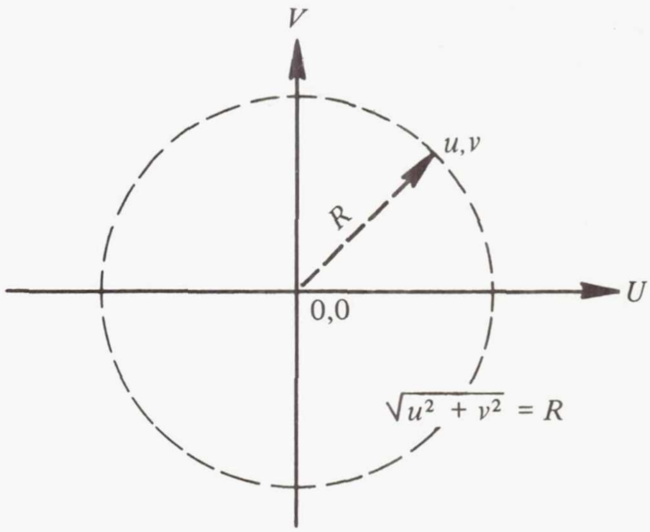

Figure 3 — Fourier transform plane.

As in the more familiar one-dimensional case, the center (0,0) corresponds to zero frequency, or dc. A blank or clear transparency would produce a point of light at (0,0) in the Fourier transform plane, since the fundamental spatial frequency of such a transparency is zero. The higher the frequency components a transparency has, the farther out from (0,0) these components will plot in the Fourier transform plane. If an opaque mask with a circular hole of radius R were placed in the U-V plane and centered at (0,0), the result would be a "spatial low-pass filter" which would eliminate all frequencies in the U-V plane where $\sqrt{u^2 + v^2} \geq R$. To illustrate the transform plane and the filtering, consider Figures 4 and 5. Figure 4 is effectively a rotated square wave. Figure 5 is the Fourier transform of Figure 4, and in it can be noted the rings corresponding to the fundamental frequency, the third, fifth, and seventh harmonics. The spot in the center corresponds to the average brightness or dc term. The rotated square wave has a Fourier series given by the equation

$$A(r) = K_2 \left[1 - \cos(K_1 r) + \frac{1}{3}\cos(3K_1 r) - \frac{1}{5}\cos(5K_1 r) + \cdots \right] ,$$

where K_2 and K_1 are constants and r is the distance from the center of the picture. The intensity of the brightness in a photograph such as Figure 4 is proportional to

$$[A(r)]^2 .$$

If there is introduced at B a mask that eliminates the rings higher than the first harmonic (a low-pass filter), the result is

$$A(r) = K_2 \left[1 - \cos(K_1 r) \right] ,$$

and the intensity is

$$I(r) = [A(r)]^2 = K_2^2 \left[1 - \cos(K_1 r) \right]^2 .$$

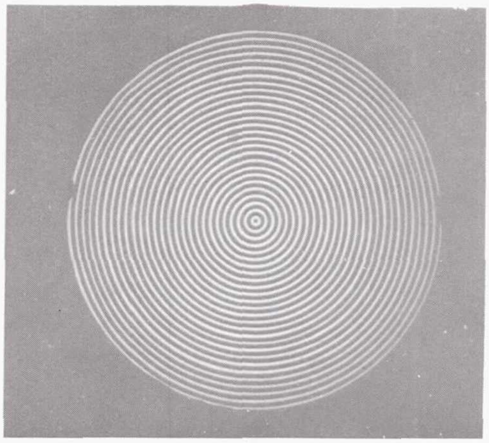

Figure 4—Rotated square wave.

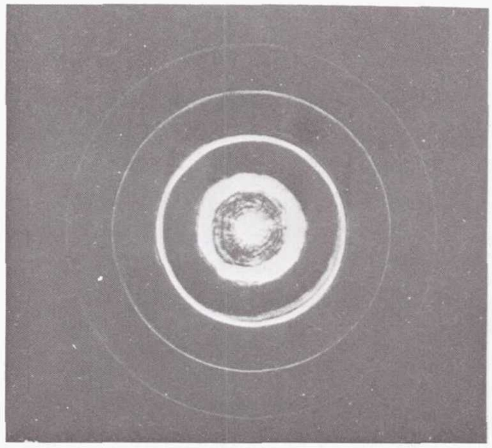

Figure 5—Fourier transform of rotated square wave.

Figure 6b shows this function compared to the original in Figure 6a. Thus we see that a removal of higher harmonics tends to blur sharp edges. If there is introduced at B a mask that eliminates the dc term and all rings higher than the third harmonic (a bandpass filter), the amplitude

$$A(r) = K_2 \left[-\cos(K_1 r) + \frac{1}{3} \cos(3K_1 r) \right] .$$

A photograph will record:

$$I(r) = [A(r)]^2 = K_2{}^2 \left[-\cos(K_1 r) + \frac{1}{3} \cos(3K_1 r) \right]^2 .$$

This is shown in Figure 7b. Note that areas which were dark in 7a (the original) are bright in 7b. When the dc component is removed, areas darker than the average brightness become negative in amplitude. When squared in the photographic process, the negative peaks become bright areas just as well as positive peaks. This is analogous to full-wave rectification. Thus "ringing" will be more likely to show up in photographs of the output than would be the case if an amplitude-sensitive device were used to record the output.

The above examples show how coherent optical techniques can be used to study the effects of "spatial frequency filtering."

APPLICATION TO INTERFEROMETER EXPERIMENT

Since, in Equation 1, $C(\mathbf{N})$ represents the Fourier transform of $D(\mathbf{P})$, the vector **N** represents points in the Fourier transform space. Limitations on **N** will therefore represent a type of "spatial frequency filtering." The magnitude of **N** has been derived by Dr. E.J. Lueke as

$$|\mathbf{N}| = \frac{2\pi f_0 d}{3 \times 10^8} , \qquad (3)$$

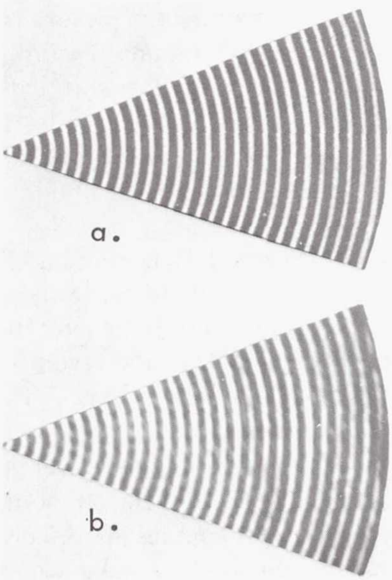

Figure 6 — Comparison of original square wave and output through low-pass filter.

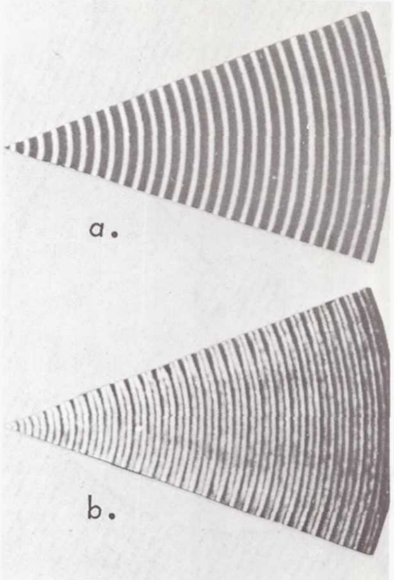

Figure 7 — Comparison of original square wave and output through bandpass filter.

from which it can be seen that $|N|$ is proportional both to the frequency f_0 of the RF source and to the distance d between the two satellites. Thus for every RF source frequency there are a maximum $|N|$ and a minimum $|N|$ corresponding, respectively, to the 3,000-meter maximum distance and the 300-meter minimum distance:

$$N_{max} = \frac{2\pi f_0 \times 3{,}000}{3 \times 10^8} \quad ,$$

$$N_{min} = \frac{2\pi f_0 \times 300}{3 \times 10^8} \quad .$$

These limitations on $|N|$ correspond to masking the function $C(N)$, whose magnitudes of $|N|$ are unlimited, with a bandpass filter with minimum frequency N_{min} and maximum frequency N_{max}.

To simulate this bandpass filter with the optical setup of Figure 2, the following experiment was performed. A two-dimensional equivalent of a unit radius celestial sphere was made. This consisted of a star pattern drawn within a circular area on a transparency. The resolution of the star pattern, or the maximum density of points in the pattern, corresponded to 20 stars per radian in the celestial sphere. The transparency was placed at A. Two masks were made in the configuration shown in Figure 8, an opaque disc being placed in the center to eliminate all spatial frequencies less than N_{min}. One mask was made to simulate N_{max} and N_{min} for 10-MHz RF sources and the other for 1-MHz RF sources. The results, recorded on film at C (Figure 2), represent the best and worst resolutions obtainable from the proposed interferometer experiment.

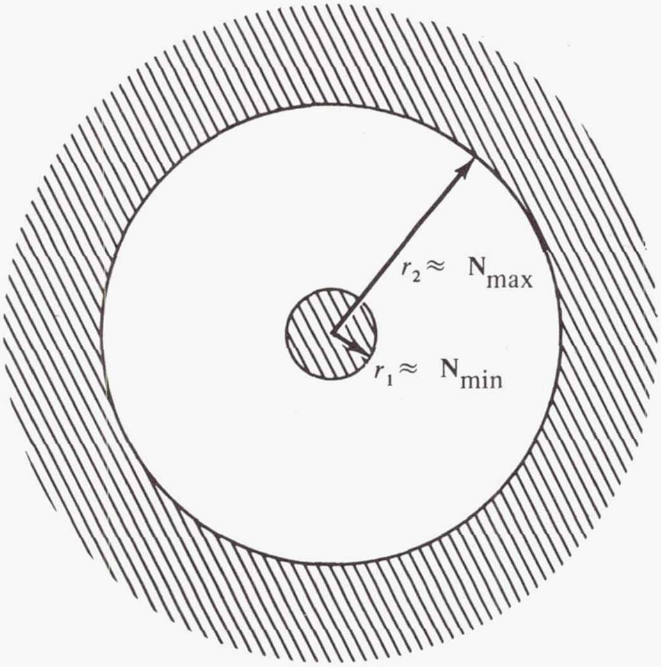

Figure 8—Mask for simulating two-dimensional bandpass filter.

Figure 9—Two-dimensional equivalent of unit radius celestial sphere.

Figure 9 shows the original star pattern. Some short lines were placed into the picture to simulate sources such as gaseous clouds. Figure 10 shows the Fourier transform of the star pattern. The outer circle, I, and the middle circle, II, in Figure 10 are N_{max} and N_{min} when the star pattern represents 10-MHz sources. The middle circle, II, and center circle, III, are N_{max} and N_{min} when the star pattern represents 1-MHz sources. Figures 11 and 12 show the results of the filtering. Figure 11 shows that bandpass limitations on 10-MHz RF sources have little effect on the resolution except for ringing around the line sources. This ringing may obliterate low-intensity point sources. Figure 12 shows that the bandpass filter had severe effects on resolution of 1-MHz RF sources. Only the most intense point sources are discernible. The line sources are smeared in most areas of the picture. One might deduce the loss of resolution for 1-MHz sources by noting the small percent of the total Fourier transform information allowed to pass through between circles II and III in Figure 10.

To determine whether the resolution might be improved if frequencies less than N_{min} were allowed, low-pass filter masks with $N_{min} = 0$ were made ($r_1 = 0$ in Figure 8). Figures 13 and 14 show the results. Figure 13 shows that, for 10-MHz sources, frequencies less than N_{min} have eliminated the ringing around the line sources. Figure 14 shows that, for 1-MHz sources, frequencies less than N_{min} have little if any effect on the resolution.

CONCLUSIONS

The main conclusions concerning the proposed radio-astronomy interferometer experiment are the following: (1) Resolution of the reconstructed star pattern is degraded by having the lower limit on the satellite separation fixed at so high a value in the plotting of RF sources frequencies near 10 MHz; (2) for resolution improvement in the 1-MHz range, the distance between the satellites must be much greater than 3,000 meters.

The simulation of this interferometer experiment is an excellent example of the ease with which coherent optics can be applied to a problem involving two-dimensional data. To do this problem on a digital computer would require long programs, large buffer memories, and input scanning devices. Coherent optics can do the job effectively with no program and no big buffers.

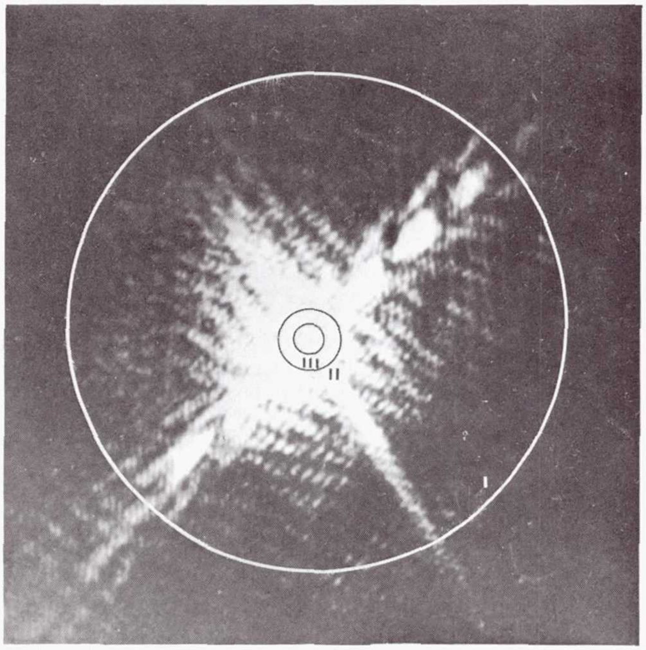

Figure 10 — Fourier transform of star pattern of Figure 9, showing relative sizes of bandpass filters.

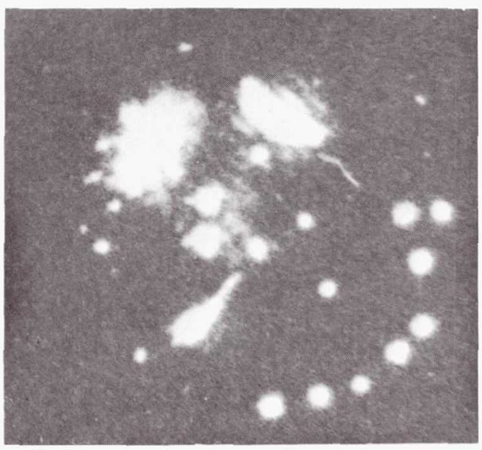

Figure 11 — Reconstructed pattern of 10-MHz RF sources through bandpass filter.

Figure 12 — Reconstructed pattern of 1-MHz RF sources through bandpass filter.

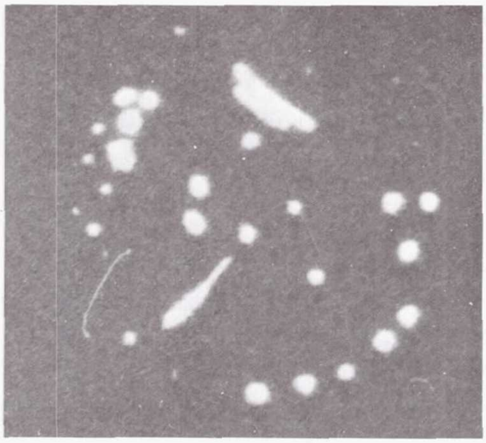

Figure 13 — Reconstructed pattern of 10-MHz RF sources when $N_{min} = 0$.

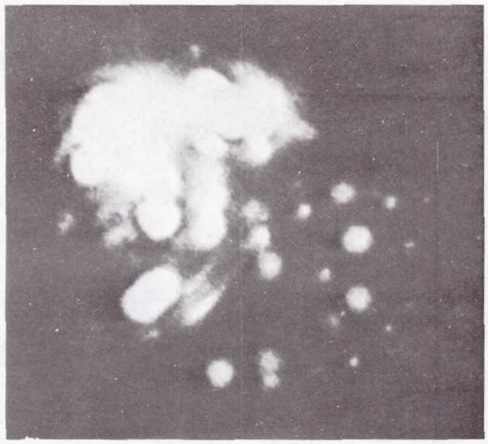

Figure 14 — Reconstructed pattern of 1-MHz RF sources when $N_{min} = 0$.

Appendix A

Mathematical Treatment of Bandpass Restrictions on the Resolution of Point Sources

The bandwidth problem mentioned in the introduction comes about from restrictions on the distance between the two satellites. The size of the antenna on the satellites limits the minimum distance to about 300 meters. Transmitter power limits the maximum distance to about 3,000 meters.

The vector **N** directed parallel to the axis connecting the two satellites has a magnitude of

$$|\mathbf{N}| = \frac{2\pi f_0 d}{c} \tag{A1}$$

which was derived by Dr. E.J. Lueke in a private communication. In this equation, f_0 is the frequency of the RF source, c is the speed of light, and d is the distance in meters between the two satellites. Thus, with the proposed restrictions on satellite separation, $|\mathbf{N}|$ is restricted between the limits corresponding to 300 meters and 3,000 meters.

In order to see mathematically the effects of these bandwidth limitations on the reconstruction of a point source, let us consider a one-dimensional case where the Fourier transform $C(\omega)$ is given by:

$$C(\omega) = \int_{-\infty}^{+\infty} f(x)\, e^{-j\omega x}\, dx \quad . \tag{A2}$$

In this equation, x is any variable, and ω is the Fourier transform variable. Let the bandwidth limitation have the form shown in Figure A1, i.e., one having a ratio of minimum to maximum frequencies of 1/10, corresponding to the 300-to-3,000 meters distance limitation.

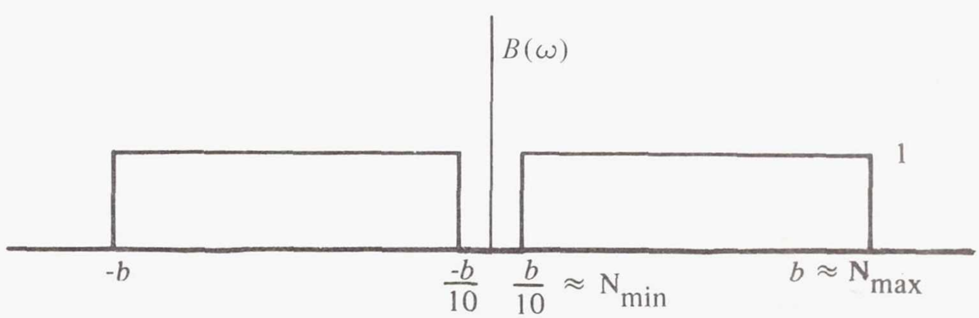

Figure A1 — Bandpass filter corresponding to N_{max} and N_{min} .

Let $f(x)$ be a Dirac delta function $\delta(x-a)$ corresponding to a point source at $x = a$. Thus the Fourier transform of the point source is (from Equation A2)

$$C(\omega) = \int_{-\infty}^{+\infty} \delta(x-a)\, e^{-j\omega x}\, dx = e^{-j\omega a} \quad .$$

The inverse Fourier transform is defined by

$$\mathrm{f}(x) = \int_{-\infty}^{+\infty} C(\omega)\, e^{j\omega x}\, d\omega \quad . \qquad \text{(A3)}$$

Taking into account the bandwidth restriction shown in Figure A1, the inverse transform for $\mathrm{f}(x)$ becomes

$$\mathrm{f}(x) = \int_{-b}^{+b} e^{-j\omega a}\, e^{j\omega x}\, d\omega - \int_{-b/10}^{+b/10} e^{-j\omega a}\, d\omega \quad ,$$

which when solved becomes

$$\mathrm{f}(x) = 2b\left[\frac{\sin b\,(x-a)}{b\,(x-a)}\right] - \frac{2b}{10}\left[\frac{\sin \dfrac{b\,(x-a)}{10}}{(x-a)}\right] \quad .$$

$\mathrm{f}(x)$ is plotted in Figure A2. From this figure it may be seen that the main brightness lobe has a width of about $\frac{2\pi}{b}$. If another point source were at a distance less than $\frac{2\pi}{b}$ from a, the main lobes in

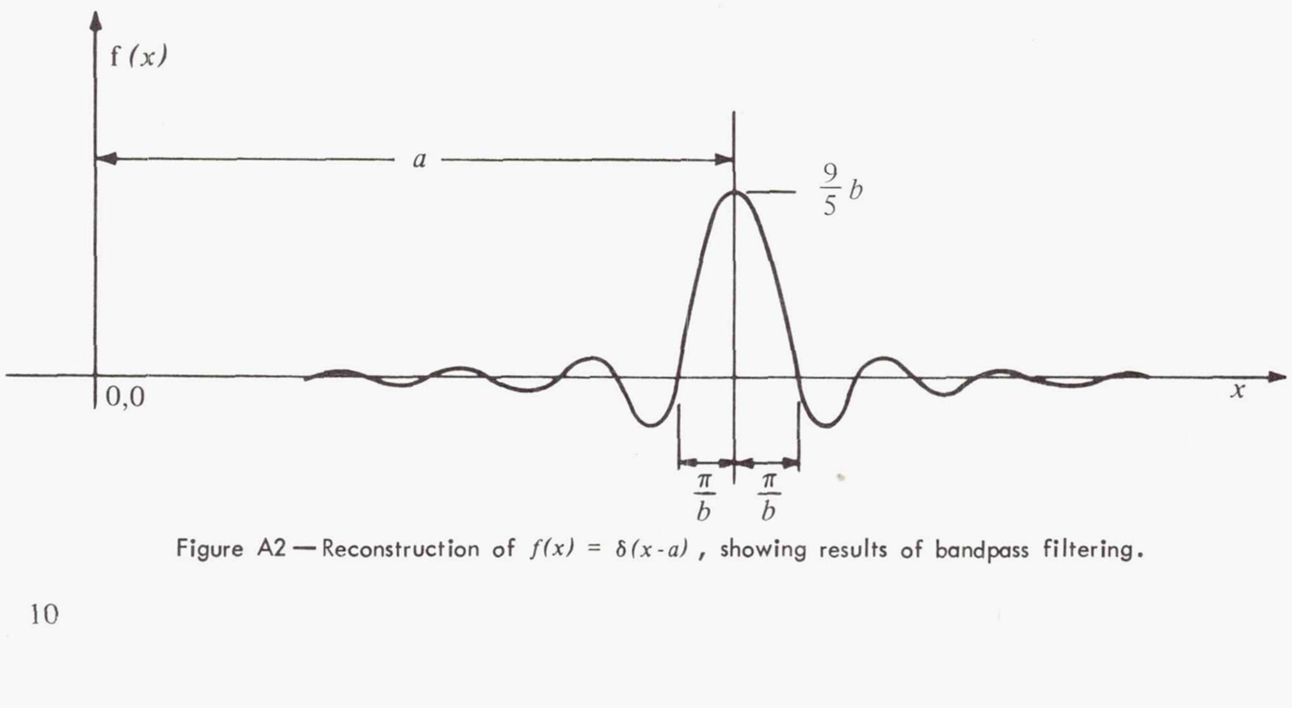

Figure A2 — Reconstruction of $f(x) = \delta(x-a)$, showing results of bandpass filtering.

the reconstruction of $f(x)$ would overlap or blur together. This main-lobe concept can be expanded to the reconstructed star pattern over the celestial sphere. Consider again Figure A1 and let $b = \mathrm{N}_{max}$. Remembering from Equation A1 that

$$\mathrm{N}_{max} = \frac{2\pi f_0 d_{max}}{c} \qquad ,$$

the main-lobe width will be:

$$\frac{2\pi}{b} = \frac{2\pi}{\dfrac{2\pi f_0 d_{max}}{c}} = \frac{c}{3{,}000\, f_0} = \frac{10^5}{f_0} \quad .$$

Thus the maximum resolution for a point source of 10 MHz will be 1/100 unit radius. Note that all dimensions are with respect to the radius of the unit celestial sphere. The 1/100 unit radius corresponds to a maximum of 100 stars per radian on the celestial sphere. For $f_0 = 1$ MHz, the maximum resolution will be 10 stars per radian.

NASA-Langley, 1969 —— 30